Polarization-resolved two-photon luminescence microscopy of V-groove arrays

Jonas Beermann,[1] Sergey M. Novikov,[1] Tobias Holmgaard,[2] René L. Eriksen,[1] Ole Albrektsen,[1] Kjeld Pedersen, [2] and Sergey I. Bozhevolnyi[1,*]

[1]*Institute of Technology and Innovation, University of Southern Denmark, Niels Bohrs Allé 1, DK-5230 Odense M, Denmark*

[2]*Department of Physics and Nanotechnology, Aalborg University, Skjernvej 4A, DK-9220 Aalborg Øst, Denmark*

[*]*seib@iti.sdu.dk*

Abstract: Using two-photon luminescence (TPL) microscopy and local reflection spectroscopy we investigate electromagnetic field enhancement effects from a μm-sized composition of 450-nm-deep V-grooves milled by focused ion beam in a thick gold film and assembled to feature, within the same structure, individual V-grooves as well as one- and two-dimensional 300-nm-period arrays of, respectively, parallel and crossed V-grooves. We analyze TPL signal levels obtained at different spatial locations and with different combinations of excitation and detection polarizations, discovering that the TPL emitted from the V-grooves is *polarized* in the direction perpendicular to that of the V-grooves. This feature implies that the TPL occurs *solely* in the form of (p-polarized) surface plasmon modes and originates therefore from the very bottom of V-grooves, where no photonic modes exist. Implications of the results obtained to evaluation of local field enhancements using TPL microscopy, especially when investigating extended structures exhibiting different radiation channels, are discussed.

OCIS codes: (250.5403) Plasmonics; (240.6680) Surface plasmons; (240.4350) Nonlinear optics at surfaces; (180.5810) Scanning microscopy.

References and links

1. J. A. Schuller, E. S. Barnard, W. Cai, Y. C. Jun, J. S. White, and M. L. Brongersma, "Plasmonics for extreme light concentration and manipulation," Nat. Mater. **9**(3), 193–204 (2010).
2. Y. Liu, C. Yu, and S. Sheu, "Low concentration rhodamine 6G observed by surface-enhanced Raman scattering on optimally electrochemically roughened silver substrates," J. Mater. Chem. **16**(35), 3546–3551 (2006).
3. K. Kneipp, Y. Wang, H. Kneipp, L. T. Perelman, I. Itzkan, R. R. Dasari, and M. S. Feld, "Single molecule detection using surfaceenhanced Raman scattering (SERS)," Phys. Rev. Lett. **78**(9), 1667–1670 (1997).
4. G. T. Boyd, Th. Rasing, J. R. R. Leite, and Y. R. Shen, "Local-field enhancement on rough surfaces of metals, semimetals, and semiconductors with the use of optical second-harmonic generation," Phys. Rev. B **30**(2), 519–526 (1984).
5. E. J. Sánchez, L. Novotny, and X. S. Xie, "Near-field fluorescence microscopy based on two-photon excitation with metal tips," Phys. Rev. Lett. **82**(20), 4014–4017 (1999).
6. K. Kneipp, H. Kneipp, I. Itzkan, R. R. Dasari, and M. S. Feld, "Surface-enhanced Raman scattering and biophysics," J. Phys. Condens. Matter **14**(18), R597–R624 (2002).
7. P. J. Schuck, D. P. Fromm, A. Sundaramurthy, G. S. Kino, and W. E. Moerner, "Improving the mismatch between light and nanoscale objects with gold bowtie nanoantennas," Phys. Rev. Lett. **94**(1), 017402 (2005).
8. P. Mühlschlegel, H.-J. Eisler, O. J. F. Martin, B. Hecht, and D. W. Pohl, "Resonant optical antennas," Science **308**(5728), 1607–1609 (2005).
9. P. Ghenuche, S. Cherukulappurath, T. H. Taminiau, N. F. van Hulst, and R. Quidant, "Spectroscopic mode mapping of resonant plasmon nanoantennas," Phys. Rev. Lett. **101**(11), 116805 (2008).
10. A. Hohenau, J. Krenn, F. Garcia-Vidal, S. Rodrigo, L. Martin-Moreno, J. Beermann, and S. Bozhevolnyi, "Spectroscopy and nonlinear microscopy of gold nanoparticle arrays on gold films," Phys. Rev. B **75**(8), 085104 (2007).
11. A. K. Sarychev and V. M. Shalaev, "Electromagnetic field fluctuations and optical nonlinearities in metal-dielectric composites," Phys. Rep. **335**(6), 275–371 (2000).
12. S. I. Bozhevolnyi, J. Beermann, and V. Coello, "Direct observation of localized second-harmonic enhancement in random metal nanostructures," Phys. Rev. Lett. **90**(19), 197403 (2003).
13. J. Beermann, I. P. Radko, A. Boltasseva, and S. I. Bozhevolnyi, "Localized field enhancements in fractal shaped periodic metal nanostructures," Opt. Express **15**(23), 15234–15241 (2007).

#158556 - $15.00 USD Received 22 Nov 2011; revised 17 Dec 2011; accepted 17 Dec 2011; published 23 Dec 2011

14. T. Søndergaard and S. I. Bozhevolnyi, "Surface-plasmon polariton resonances in triangular-groove metal gratings," Phys. Rev. B **80**(19), 195407 (2009).
15. T. Søndergaard, S. I. Bozhevolnyi, J. Beermann, S. M. Novikov, E. Devaux, and T. W. Ebbesen, "Resonant plasmon nanofocusing by closed tapered gaps," Nano Lett. **10**(1), 291–295 (2010).
16. J. Beermann, S. M. Novikov, T. Søndergaard, J. Rafaelsen, K. Pedersen, and S. I. Bozhevolnyi, "Localized field enhancements in two-dimensional V-groove metal arrays," J. Opt. Soc. Am. B **28**(3), 372–378 (2011).
17. A. Mooradian, "Photoluminescence of metals," Phys. Rev. Lett. **22**(5), 185–187 (1969).
18. G. T. Boyd, Z. H. Yu, and Y. R. Shen, "Photoinduced luminescence from the noble metals and its enhancement on roughened surfaces," Phys. Rev. B Condens. Matter **33**(12), 7923–7936 (1986).
19. M. R. Beversluis, A. Bouhelier, and L. Novotny, "Continuum generation from single gold nanostructures through near-field mediated intraband transitions," Phys. Rev. B **68**(11), 115433 (2003).
20. A. Bouhelier, M. R. Beversluis, and L. Novotny, "Characterization of nanoplasmonic structures by locally excited photoluminescence," Appl. Phys. Lett. **83**(24), 5041–5043 (2003).
21. K. Imura, T. Nagahara, and H. Okamoto, "Near-field two-photon-induced photoluminescence from single gold nanorods and imaging of plasmon modes," J. Phys. Chem. B **109**(27), 13214–13220 (2005).
22. R. A. Farrer, F. L. Butterfield, V. W. Chen, and J. T. Fourkas, "Highly efficient multiphoton-absorption-induced luminescence from gold nanoparticles," Nano Lett. **5**(6), 1139–1142 (2005).
23. A. Bouhelier, R. Bachelot, G. Lerondel, S. Kostcheev, P. Royer, and G. P. Wiederrecht, "Surface plasmon characteristics of tunable photoluminescence in single gold nanorods," Phys. Rev. Lett. **95**(26), 267405 (2005).
24. J. Beermann, S. M. Novikov, T. Søndergaard, A. E. Boltasseva, and S. I. Bozhevolnyi, "Two-photon mapping of localized field enhancements in thin nanostrip antennas," Opt. Express **16**(22), 17302–17309 (2008).
25. J. Beermann, S. M. Novikov, K. Leosson, and S. I. Bozhevolnyi, "Surface enhanced Raman imaging: periodic arrays and individual metal nanoparticles," Opt. Express **17**(15), 12698–12705 (2009).
26. Q.-Q. Wang, J.-B. Han, D.-L. Guo, S. Xiao, Y.-B. Han, H.-M. Gong, and X.-W. Zou, "Highly efficient avalanche multiphoton luminescence from coupled Au nanowires in the visible region," Nano Lett. **7**(3), 723–728 (2007).
27. Z.-K. Zhou, X.-N. Peng, Z.-J. Yang, Z.-S. Zhang, M. Li, X.-R. Su, Q. Zhang, X. Shan, Q.-Q. Wang, and Z. Zhang, "Tuning gold nanorod-nanoparticle hybrids into plasmonic Fano resonance for dramatically enhanced light emission and transmission," Nano Lett. **11**(1), 49–55 (2011).
28. T. Søndergaard, S. I. Bozhevolnyi, S. M. Novikov, J. Beermann, E. Devaux, and T. W. Ebbesen, "Extraordinary optical transmission enhanced by nanofocusing," Nano Lett. **10**(8), 3123–3128 (2010).
29. J. Beermann, T. Søndergaard, S. M. Novikov, S. I. Bozhevolnyi, E. Devaux, and T. W. Ebbesen, "Field enhancement and extraordinary optical transmission by tapered periodic slits in gold films," New J. Phys. **13**(6), 063029 (2011).
30. A. Aubry, D. Y. Lei, A. I. Fernández-Domínguez, Y. Sonnefraud, S. A. Maier, and J. B. Pendry, "Plasmonic light-harvesting devices over the whole visible spectrum," Nano Lett. **10**(7), 2574–2579 (2010).
31. M. D. Wissert, K. S. Ilin, M. Siegel, U. Lemmer, and H.-J. Eisler, "Coupled nanoantenna plasmon resonance spectra from two-photon laser excitation," Nano Lett. **10**(10), 4161–4165 (2010).

1. Introduction

Electromagnetic interactions in nanostructured materials and, especially, in metal nanostructures give rise to various fascinating optical phenomena. One of the main research directions in nano-optics is the search for configurations that efficiently interconvert propagating (μm-sized) and strongly localized (nm-sized) optical fields resulting thereby in strongly enhanced local fields, which are indispensable for optical characterization, sensing and manipulation at nanoscale [1]. Realization of field enhancement (FE) that enforces surface enhanced Raman scattering (SERS) is extremely important for highly sensitive detection of low molecular concentrations [2], ultimately reaching the limit of single molecule detection [3]. In this perspective, metal nanostructures supporting surface plasmon (SP) resonances have been intensively investigated with respect to achieving strong FE effects [1]. An important research direction is thereby the design of metal nanostructures that ensure well-pronounced SP resonances within a given wavelength range along with substantial and robust (with respect to fabrication inaccuracies) FE. Several strategies have already been suggested and pursued, dealing with various shapes and configurations of metal nanostructures, ranging from individual pointed particles [4, 5] to their pairs [6–9] and periodic [10] as well as random [11, 12] and fractal shaped [13] ensembles.

Large FE occurring due to SP resonances in one-dimensional (1D) V-groove metal gratings has very recently been treated theoretically [14] and demonstrated experimentally with individual V-grooves milled in gold [15]. The achieved enhancements depend on the geometry of each individual V-groove (i.e., depth and opening angle) [15] as well as on the separation between V-grooves interacting in 1D gratings [14]. By this means the FE can be

#158556 - $15.00 USD Received 22 Nov 2011; revised 17 Dec 2011; accepted 17 Dec 2011; published 23 Dec 2011

tuned in the wavelength range from visible to infrared, making this configuration promising for a wide range of practical applications, e.g., within surface-enhanced spectroscopies. The periodic V-groove arrangement further increases the interaction and FE via SP polaritons (SPPs) reflected between the grooves, provided that the periodicity is optimized so that standing-wave SPP resonances would coincide with localized (shape-dependent) SP resonances of individual V-grooves [14–16].

One well-established experimental technique for evaluation of FE related to metal nanostructures is two-photon induced photoluminescence (TPL), which was earlier described [17–23], with spatially resolved TPL studies [9, 19] and near-field imaging [20, 21] used for characterization of local FE levels. We have previously used TPL signals in scanning optical microscopy for estimations of the local FE factor achieved with various types of samples, such as individual metal nanostrips [24], periodic metal nanoparticles [10], and fractal shaped metal nanostructures [13]. The main goal in these experiments was to realize SP resonances in predesigned wavelength ranges and characterize local FE factors aiming at obtaining strong and robust FE effects that are of great importance for surface-enhanced spectroscopies, especially for local SERS [25]. Strong SP resonances in gold nanostructures can also result, under intense illumination, in avalanche multiphoton-induced photoluminescence [8, 26, 27]. It should be noted that, in most of the above experiments, the polarization of the detected TPL was not analyzed bearing in mind that luminescence is generally incoherent (and unpolarized) and following the widely accepted approach [7, 8] of FE evaluation by comparing TPL signals from a flat metal surface and nanostructure in question. Nevertheless, influence of the detected TPL polarization on the appearance of TPL images has been noted [13] and explained by the circumstance that the TPL radiation (originating from locations of FE) interacts with the immediate scattering environment that can influence the TPL scattering in the direction of its detection [10, 13].

In this work, using polarization-resolved TPL microscopy (i.e., recording TPL images with different combinations of excitation and detection polarizations) in combination with spatially-resolved linear reflection spectroscopy, we investigate a 7×7-μm^2-sized structure composed of 450-nm-deep V-grooves milled by focused ion beam (FIB) in a thick gold film and assembled to feature, within the same configuration, individual V-grooves as well as one- and two-dimensional 300-nm-period arrays of parallel and crossed V-grooves (Fig. 1). Differently oriented (individual and grouped) V-grooves allow us to directly compare TPL signals obtained for *different* polarization configurations and local environment by using the same TPL image, i.e., at the *same* illumination and detection conditions. In addition, linear reflection images, by revealing the radiation absorption at the illumination wavelength, elucidate interplay between FE effects and TPL generation.

Note again that for the previously investigated similar structures, such as tapered gaps [15, 16] and periodic slits [28, 29], we have used the *unpolarized* detection (i.e., without an analyzer in front of a detector) of generated TPL in order to maximize the recorded signal-to-noise ratio. Usually, this is a reasonable procedure since luminescence is an incoherent process without preferred polarization, and detecting only a certain polarization would normally not add additional information except for merely decreasing overall signal levels. However, for V-grooves supporting only *p*-polarized SPP modes and we expect main TPL contributions originating at the narrow bottom, it turns out to be very interesting to investigate the polarization properties of TPL reaching a detector (in the far-field). Polarization-resolved TPL microscopy used in the present work provides a clear evidence of TPL occurring *solely* in the form of *p*-polarized (perpendicular to the groove direction) SPP modes and originating therefore from the very bottom of V-grooves, where no photonic modes exist. Essentially, we thereby *experimentally* demonstrate that the strongest FE (and generated TPL) is indeed located in a small region close to the bottom of V-groove, a conjecture that was widely used in our previous research being based on theoretical considerations [15, 16, 28, 29].

In order to collect and send as much light as possible toward the bottom of the grooves we fabricate practically touching V-grooves with walls curving toward the groove tip and meeting with a vanishingly small angle [Fig. 1(b)], ending up with a configuration that is

#158556 - $15.00 USD Received 22 Nov 2011; revised 17 Dec 2011; accepted 17 Dec 2011; published 23 Dec 2011

somewhat similar to the so-called kissing nanowires [30]. However, here we implement the V-groove geometry with the purpose to investigate the FE effect when moving from individual V-grooves into a parallel 1D set and, finally, a 2D array of *crossing* V-grooves. Accordingly, we observed the effect of individual, 1D and 2D V-groove configurations in the same structure and with fixed parameters of depth and spacing between the V-grooves thereby rendering TPL measurements of different areas in the same scan to be directly comparable.

2. Sample and experimental setup

The sample consists of five V-grooves written by FIB (Zeiss 1540 XB) along the x-direction and five V-grooves written along the y-direction and crossing the others at the center as imaged by scanning electron microscopy (SEM) [Fig. 1(a)]. For both the vertical (along y) and horizontal (along x) V-grooves, the central one is 7 μm long, whereas the others are 4 μm long. The spacing between parallel V-grooves is 300 nm and each has a depth of ~450 nm. The grooves are fabricated using 20 pA milling current with initially 3 line runs along each groove for the horizontal and vertical directions all at the same dose, followed by additionally 1 line run at the same dose along the horizontal grooves and finally 1 line run with only 50% dose along the vertical grooves. This procedure was introduced after repeated testing in order to obtain the deepest V-grooves at relatively narrow spacing and with the best similarity and symmetry between the horizontal and vertical written grooves, which could be an issue due to material re-deposition at the initially written V-grooves. The zoomed SEM image reveals a good structure quality and with relatively deep V-grooves in both directions and forming pointy ellipsoids at the intersections, i.e., with no flat area between the grooves [Fig. 1(b)].

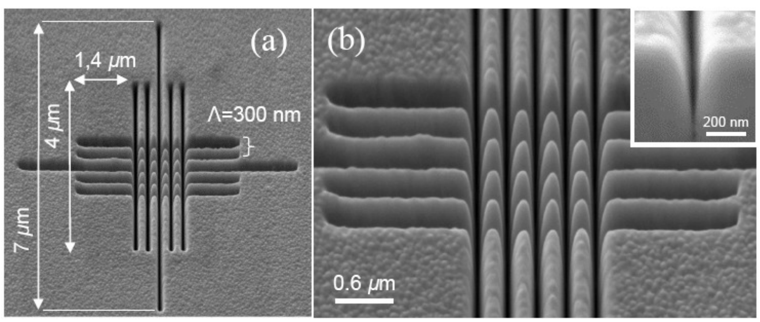

Fig. 1. (a) Overview and (b) zoomed SEM images (taken at a tilt angle of 54° with respect to normal incidence) of the FIB fabricated structure of crossing V-grooves having a groove period Λ = 300 nm and depth d = 450 nm. Inset in (b) shows a similarly obtained SEM image of a cut through an individually V-groove milled under the same conditions.

Scattering properties of the fabricated crossing V-grooves were studied using spatially-resolved linear reflection spectroscopy. The spectroscopic reflection analysis was performed on a BX51 microscope (Olympus) equipped with a halogen light source, polarizers and a fiber-coupled grating spectrometer QE65000 (Ocean Optics) with a wavelength resolution of 1.6 nm. The reflected light was collected in backscattering configuration using MPlanFL (Olympus) objective with magnification × 100 (NA = 0.9). The image area analyzed by the spectrometer is limited by a pinhole with a diameter of 150 μm resulting in a circular probing area with a diameter of 1.5 μm. The microscope images (1600 × 1200 pixels) were captured with a LC20 digital color camera (Olympus) [Fig. 2(a)-2(b)].

The FE levels obtained with an individual V-groove, as well as with 1D and 2D configurations of V-grooves were characterized by TPL microscopy. Our experimental setup for TPL has been described in detail previously [15, 16, 29]. It consists of a scanning optical microscope in reflection geometry built on the base of a commercial microscope and a computer-controlled two-dimensional piezoelectric translation stage. The linearly polarized light beam from a mode-locked pulsed (pulse duration ~200 fs, repetition rate ~80 MHz) Ti-Sapphire laser (wavelength λ = 730 – 790 nm, $\delta\lambda$ ~10 nm, average power ~300 mW) is used

#158556 - $15.00 USD Received 22 Nov 2011; revised 17 Dec 2011; accepted 17 Dec 2011; published 23 Dec 2011

as a source of sample illumination at the fundamental harmonic (FH) frequency. After passing an optical isolator (to avoid back-reflection), half-wave plate, polarizer and wavelength selective beam splitter, the laser beam is focused on the sample surface at normal incidence with a Mitutoyo infinity-corrected × 100 objective (NA = 0.7). The TPL radiation generated in reflection and the reflected FH beam are collected with the same objective, separated by a beam splitter, directed through appropriate filters and polarizers and detected with two photomultiplier tubes, the tube for TPL photons (within the transmission band of 350-550 nm) being connected with a photon counter. The FH and TPL resolution at full-width-half-maximum were ~0.75 μm and ~0.35 μm, respectively. In this work, we used the following scan parameters: the integration time (at one point) of 100 ms, speed of scanning (between the measurement points) of 20 μm/s, scan area of 8 × 8 μm^2, and scanning step size of 100 nm. We adjusted the incident power P within the range 0.7-2.5 mW in order to obtain significant TPL signals (typically, ~100 counts/s). It has also been checked that TPL signals depended quadratically on the incident power as expected for the two-photon induced up-conversion.

3. Results and discussion

The SPs modes in the V-groove can be excited only for *p*-polarized incident electric fields, i.e., here with the electric field being perpendicular (and the magnetic field parallel) to the V-grooves [15]. On the other hand, *s*-polarized light, with the electric field parallel to the V-grooves, is almost completely reflected because its penetration experiences cutoff with respect to the groove width, since no photonic modes can propagate down beyond the groove width that is less than half of the light wavelength and no SPs modes exist in the groove for *s*-polarization. Optical images of the crossing V-grooves obtained for different polarizations of the detected light clearly demonstrate this phenomenon [Fig. 2(a), 2(b))].

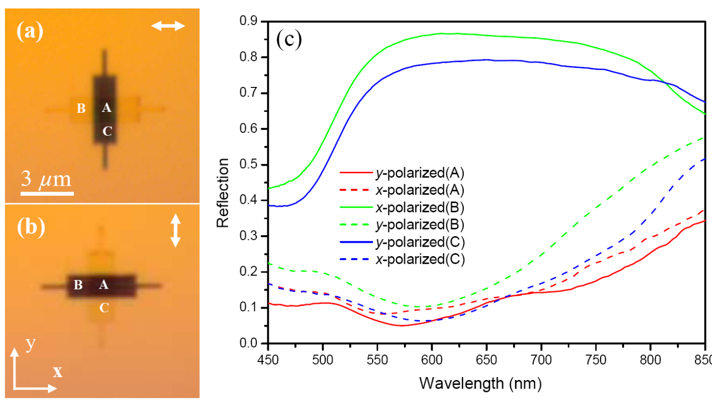

Fig. 2. Optical images of the crossing V-grooves with the groove period of 300 nm and depth of 450 nm obtained for (a) *x*- and (b) *y*-polarized detection as indicated by double arrows (Media 1). (c) Reflection spectra of the crossing V-grooves sample obtained for *x*- and *y*-polarization in the positions marked by letters A, B, C in (a) and (b). Optical image (b) is linked with the movie (3640KB) showing the image evolution with the rotation of analyzer.

Using the *x*-polarized light one can see only the vertical 1D part of the crossing V-grooves and for *y*-polarized light only the horizontal 1D parts, whereas for both cases the 2D center of the sample is visible and actually appears slightly darker. Turning to the spatially-resolved linear reflection spectroscopy described above, we were able to obtain local spectra [Fig. 2(c)] for both *x*- and *y*-polarized detection from within a 1.5-μm-diameter spot at the center [letter A in Fig. 2(a), 2(b)], where V-grooves intersect - forming a 2D configuration, as well as at the horizontal (letter B) and vertical (letter C) positions with 1D V-grooves. The experimental data in Fig. 2(c) represent the reflection ratio R_{str}/R_{ref}, where R_{str} is the reflection measured from the structure and R_{ref} is the reference spectrum recorded from the smooth gold surface. The *x*-polarized incident light experiences almost full reflection from area B, whereas the reflection dramatically decreases in areas A and C [Fig. 2(c)]. On the other hand, the *y*-

#158556 - $15.00 USD Received 22 Nov 2011; revised 17 Dec 2011; accepted 17 Dec 2011; published 23 Dec 2011

polarized light gives the reverse situation - with almost full reflection in area C and low reflection in area B, whereas the reflection level from the center (area A) remains very low as for the *x*-polarized light [Fig. 2(c)]. It should be noted, that the reflection from the central part of the sample for both polarizations is even less than from areas C for *x*-polarization and B for *y*-polarization. We think that the phenomena of broadband reflection suppression observed for 1D and 2D arrays of V-grooves (indicating substantial light absorption) might be similar in underlying physics to that described theoretically for touching nanowires [30]. Here it should be emphasized that the V-groove array period of 300 nm was specifically chosen to be sufficiently small so as to exclude the influence grating diffraction effects, e.g., Rayleigh anomalies [14], on the reflection spectra.

In order to characterize the local FE of the crossing V-grooves we used the TPL microscopy described above to obtain both FH [Fig. 3(a), 3(b)] and TPL images [Fig. 3(c), 3(d)] of the cross structure. As expected the FH images exhibit good correlation with the results obtained in white light illumination [Fig. 2(a), 2(b)) and insets in Fig. 3(a, b)]. Likewise, the polarized TPL images exhibit bright areas (highest TPL signals) at the locations corresponding to V-grooves being excited in a *p*-polarized configuration, but with an improved contrast and larger differences observed between the individual, 1D and 2D locations. One fine detail is that, for each of the TPL bright V-groove directions, the TPL images are actually slightly asymmetric along the V-groove with respect to the 2D center of the structure, i.e., the top part of Fig. 3(c) and right side of Fig. 3(d). This can be explained by a slight variation in the groove width and depth at the end of the FIB writing of each V-groove as demonstrated by a detailed normal incidence SEM image of a test structure with 5 parallel V-grooves fabricated in only one direction [Fig. 3(e)]. For this test structure the FIB fabrication along each groove was starting from the left and ending to the right, where it is clear that the grooves are both wider and deeper than to the left [Fig. 3(e)]. This is probably caused by ongoing re-deposition at the bottom and sides of the V-groove, which is then not the case at the very end of each FIB written line. A more open V-groove is likely to facilitate both increased excitation of SP groove modes and emission of TPL generated at the narrow bottom. Accordingly, we obtain slightly higher TPL signals at those ends of the V-grooves where each line in the FIB writing was terminated and thereby causing more open V-grooves due to less re-deposition. In hindsight, one could most likely have reduced these effects of less re-deposition at one end by systematical changing the writing direction between each FIB line, a procedure that one should definitely try out in future investigations.

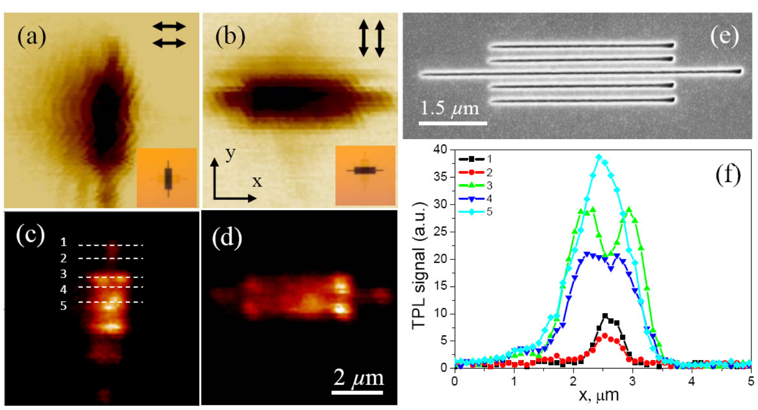

Fig. 3. (a), (b) FH and (c), (d) TPL images of the crossing V-grooves with groove period 300 nm and depth 450 nm obtained at λ = 740 nm for (a), (c) *x*- and (b), (d) *y*-polarized excitation and detection as indicated by double arrows. (e) SEM image of a test area with only a 1D structure exhibiting slightly wider grooves at one end caused by less re-deposition during the last part of each FIB-written line along the groove. (f) Averaged and normalized TPL signal cross sections taken at the positions indicated by white lines numbered in (c) and corresponding to the cross section number labeled in (f). Insets in (a), (b) show optical images obtained for the same polarization as indicated in (a), (b) by double arrows.

#158556 - $15.00 USD Received 22 Nov 2011; revised 17 Dec 2011; accepted 17 Dec 2011; published 23 Dec 2011

Since the sample configuration is tailored for simultaneous TPL characterization of structures resembling individual V-grooves, as well as 1D and 2D V-groove arrays, one still has a good possibility to quantitatively compare the TPL signals and estimate the degree of FE. One option is to obtain averaged TPL signals in cross-sections at the positions indicated by white dashed lines in Fig. 3(c). These cross-sections [Fig. 3(f)] show clearly different levels in the TPL intensity variation across the SP excited V-grooves: the TPL signal is relatively small for the individual groove (black and red curves), increasing for the 1D array (blue and green curves) and reaching maximum for 2D arrays at the center of intersecting V-grooves (cyan curves) [Fig. 3(f)]. The largest TPL signals observed are comparable to those obtained in the previous experiments with individual [15] and 2D periodic [16] V-grooves. However, in view of our observations reported below, we decided to abstain from evaluations of FE levels from TPL signals using the previously used approach [15, 16].

First we note that the TPL intensity measured in the cross-sections at the ends of the individual (black curve) and 1D grooves (green curves) is slightly higher compared to the intermediate positions (red and blue), a feature that is in accordance with the end-effects and visual inspection of the TPL images mentioned above. The fact that the central 2D part of the cross exhibits higher TPL signals compared with the 1D parallel grooves is believed to be due to the main TPL origin being the narrow bottom of the V-grooves which is only accessible via SP modes. At the intersections there is, however, an increased possibility of also photonic modes actually accessing the bottom of the structure, as well as some additional signal caused by pointy ellipsoids formed at these intersections [Fig. 1(b)]. Images obtained in white light illumination [Fig. 4(a)] and TPL [Fig. 4(b)] when using the cross-polarized configuration of FH excitation and detection demonstrate these phenomena more clearly.

The TPL signal, obtained for the cross-polarized configuration indicated [Fig. 4(b)], is visible only from the central 2D part of the structure and has relatively low intensity compared to the levels obtained with the parallel excitation and detection polarization [Fig. 3(c)-(d)]. Only the 2D structure shows up in the cross-polarized configuration with the excitation along the y- and detection along x-axis, since the 1D V-groove orientation along the y-axis does not allow proper p-polarized SP excitation *inside* the grooves, whereas the perpendicular 1D V-groove orientation (along the x-axis) does. However, the TPL *emitted* from the latter and propagating toward a detector is y-polarized (the TPL can only escape from the narrow V-groove bottom via p-polarized SP modes) and thus blocked by an analyzer. In short, for the y-polarized illumination and x-polarized detection, TPL in y-oriented V-grooves cannot be excited whereas TPL excited in x-oriented V-grooves cannot be detected. In the central area of crossing V-grooves, both incident FH and emitted TPL radiation become depolarized due to scattering by pointy ellipsoids [Fig. 1(a)] resulting in (relatively weak, but nonzero) TPL excitation in y-oriented V-grooves and detection of TPL excited in x-oriented V-grooves. In addition, non-polarized TPL can also be produced by the pointy ellipsoids remaining at the V-groove intersections. The averaged TPL signal in the cross section indicated by the white dashed line in the TPL image confirms that the TPL is relatively low and present only from the (1.6×1.6 μm^2)-area with 2D V-groove structures [Fig. 4(c)]. Consequently, the maximum TPL signal obtained with cross-polarization is only ~7.5 compared to the level of ~40 obtained with the parallel polarization configuration [cf. Figure 4(c) and Fig. 3(f)], demonstrating clearly that, in *contrast* to the usual luminescence properties, the TPL emitted from V-grooves is highly polarized. It should be noted that the polarized TPL emission was also observed in the experiments with crystalline gold nanorods, in which the TPL polarization characteristics have been related to the crystalline and band structures of the investigated gold nanorods [21].

#158556 - $15.00 USD Received 22 Nov 2011; revised 17 Dec 2011; accepted 17 Dec 2011; published 23 Dec 2011

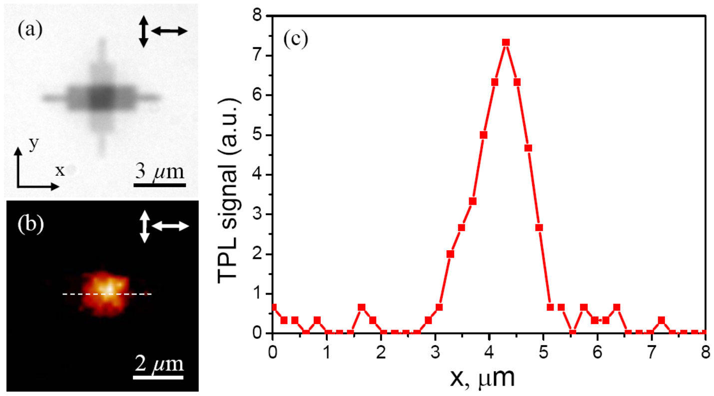

Fig. 4. (a) White light and (b) TPL images of the crossing V-grooves with period 300 nm and depth 450 nm obtained at λ = 740 nm in cross-polarized configuration, i.e., with the *y*-polarized excitation and *x*-polarized detection as indicated by double arrows, along with (c) averaged TPL signal in the cross section taken across the sample as indicated by a white line in (b).

To further investigate and confirm these polarization properties of the TPL emitted from V-grooves we have also performed the polarization-resolved TPL microscopy of an individual V-groove using both parallel and cross-polarized TPL detection (Fig. 5). We have used the sample fabricated previously and used for studies of resonant plasmon nanofocusing [15], containing several straight 150-μm-long V-grooves with opening angles close to 28 degrees and depths of 1.1-1.3 μm that were FIB-milled in a 1.8-μm-thick gold layer. As seen from both the obtained FH [Fig. 5(a)] and TPL images [Fig. 5(b, c)], the selected individual V-groove clearly contains two defects, most probably gold corns, which appear as dark spots in the FH image (due to reduced back reflection) and very bright spots in the TPL images. As illustrated by the obtained TPL signal in the cross sections [Fig. 5(d)] the FH reflection minimum corresponds to the position of high TPL intensity for *p*-polarized light. In the case of using the cross-polarized detection along the *x*-axis (detecting thereby only the *s*-polarized TPL emission from the V-groove) [Fig. 5(c)], we end up extinguishing the TPL signal along the entire V-groove except at the two defects, which appear similarly bright in both cross-polarized and parallel detection configurations [Fig. 5(b)-(c)]. The latter feature is most probably related to the circumstance that these defects are located sufficiently close to the V-groove opening so that the corresponding TPL can escape the groove via photonic modes. All in all, we believe that the above observations of an individual V-groove with defects is a crucial experiment demonstrating *directly* that the TPL emitted from V-grooves (without defects) is associated with strong FE localized to a *small (nm-sized)-volume* at the very bottom of V-grooves (and not merely emitted from the sidewalls or top edges along the V-groove), and verifying thereby the conjecture used in our previous research [15,16,28,29].

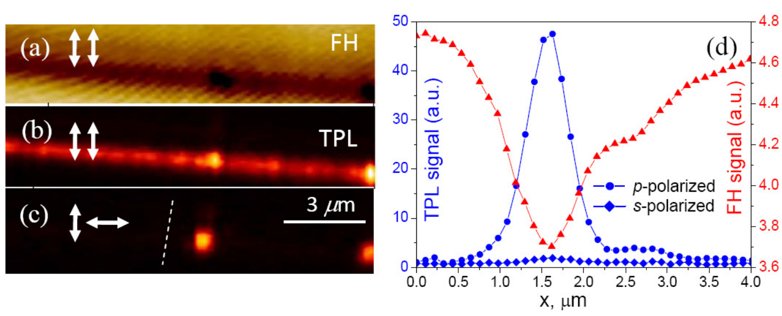

Fig. 5. (a) FH and (b), (c) TPL images of an individual 1.1-1.3 μm deep V-groove with a small defect obtained at λ = 750 nm for (a),(b) parallel *p*-polarized excitation and detection and (c) crossed *p*-polarized excitation and *s*-polarized detection as indicated by double arrows. (d) Averaged TPL signal in the cross section indicated by a white line in (c).

#158556 - $15.00 USD Received 22 Nov 2011; revised 17 Dec 2011; accepted 17 Dec 2011; published 23 Dec 2011

Our findings indicate that the generally accepted and widely used approach of FE evaluation by comparing TPL signals from a flat metal surface and nanostructure in question [7, 8] should be used with great care, especially when investigating extended structures exhibiting different radiation channels. It is clear that, as also noted previously [10, 13], one should take into account that the *detected* TPL radiation is determined not only by local FE at the illumination wavelength but also by the immediate scattering environment selecting, i.e., enhancing or suppressing, particular TPL polarizations and wavelengths. It has already been observed that the TPL emission spectra match dark-field microscopy scattering spectra obtained with individual [23] and, more recently, coupled [31] gold nanorods, indicating thereby that the TPL efficiency can be *enhanced* by plasmonic resonances at TPL wavelengths. On the other hand, for the considered configuration, TPL escaping from V-grooves in the form of SP modes should be expected to reflect SP propagation *losses* that are strongly wavelength dependent. In any case, TPL wavelength and polarization dependent enhancement/loss on the way from FE locations to a remote detector should be incorporated in the procedure of FE evaluation. Furthermore, it should also be borne in mind that TPL signals are related to electromagnetic fields formed *inside* (irradiated) gold nanostructures [10], so that the FE determined from TPL measurements should be used with great care when considering phenomena such as, for example, SERS from adsorbed molecules, which are related to electromagnetic fields formed *outside* illuminated gold structures, i.e., in their immediate dielectric environment [25]. Even though electromagnetic fields inside and outside of gold nanostructures are directly related via the boundary conditions, the relation between inside and outside FE factors is quite complicated due to (often) unknown polarization characteristics of the electromagnetic fields in question [10].

4. Conclusion

Summarizing, using polarization-resolved TPL microscopy and spatially-resolved reflection spectroscopy we have investigated electromagnetic FE effects from a μm-sized composition of 450-nm-deep V-grooves milled by focused ion beam in a thick gold film and assembled to feature, within the same structure, individual V-grooves as well as one- and two-dimensional 300-nm-period arrays of, respectively, parallel and crossed V-grooves. We have analyzed TPL signal levels obtained at different spatial locations and with different combinations of excitation and detection polarizations, discovering that the TPL emitted from the V-grooves is *polarized* in the direction perpendicular to that of the V-grooves. This feature has been related to the circumstance that the TPL occurs *solely* in the form of (p-polarized) surface plasmon modes and originates therefore from the very bottom of V-grooves, where no photonic modes exist. We have also discussed implications of the results obtained to evaluation of local FE using TPL microscopy and applying the widely used approach, in which FE is estimated by comparing TPL signals from a flat metal surface and given nanostructure. Additionally, we have observed efficient broadband and polarization independent absorption of radiation incident on the (central) area containing the 300-nm-period array of perpendicular oriented 450-nm-deep V-grooves. We believe that our findings are important for a number of plasmonic applications such as surface-enhanced Raman spectroscopy and photovoltaics.

Acknowledgments

The authors gratefully acknowledge financial support from the Danish Council for Independent Research (FTP contract no. 09-072949) and the Lundbeck Foundation (contract no. R49-A5871). The authors thank P. K. Kristensen and J. Rafaelsen (Aalborg University) for assistance in the sample fabrication.